The effects of footplate stiffness on push-off power when walking with posterior leaf spring ankle-foot orthoses

Kerkum, Y. L.; Philippart, W.; Houdijk, H.

Published in:
Clinical Biomechanics

DOI:
10.1016/j.clinbiomech.2021.105422

Clinical Biomechanics 88 (2021) 105422

Contents lists available at ScienceDirect

Clinical Biomechanics

journal homepage: www.elsevier.com/locate/clinbiomech

The effects of footplate stiffness on push-off power when walking with posterior leaf spring ankle-foot orthoses

Y.L. Kerkum [a,b,*], W. Philippart [c], H. Houdijk [c,d]

[a] REVAL Rehabilitation Research Center, Faculty of Rehabilitation Sciences, Hasselt University, Diepenbeek, Belgium
[b] Research and Development, OIM Orthopedie, Assen, the Netherlands
[c] Department of Human Movement Sciences, Faculty of Behaviour and Movement Sciences, Amsterdam Movement Sciences, Vrije Universiteit Amsterdam, Amsterdam, the Netherlands
[d] University of Groningen, University Medical Center Groningen, Center for Human Movement Sciences, Groningen, the Netherlands

A R T I C L E I N F O

Keywords:
Gait
Biomechanics
Ankle-foot orthoses
Material properties
Foot model

A B S T R A C T

Background: Many studies on ankle-foot orthoses investigated the optimal stiffness around the ankle, while the effect of footplate stiffness has been largely ignored. This study investigated the effects of ankle-foot orthosis footplate stiffness on ankle-foot push-off power during walking in able-bodied persons.
Methods: Twelve healthy participants walked at a fixed speed (1.25 $m \cdot s^{-1}$) on an instrumented treadmill in four conditions: shod and with a posterior leaf-spring orthosis with a flexible, stiff or rigid footplate. For each trial, ankle kinematics and kinetics were averaged over one-minute walking. Separate contributions of the ankle joint complex and distal hindfoot to total ankle-foot power and work were calculated using a deformable foot model.
Findings: Peak ankle joint power was significantly higher with the rigid footplate compared to the flexible and stiff footplate and not different from shod walking. The stiff footplate increased peak hindfoot power compared to the flexible and rigid footplate and shod walking. Total ankle-foot power showed a significant increase with increasing footplate stiffness, where walking with the rigid footplate was comparable to shod walking. Similar effects were found for positive mechanical work.
Interpretation: A rigid footplate increases the lever of the foot, resulting in an increased ankle moment and energy storage and release of the orthosis' posterior leaf-spring as reflected in higher ankle joint power. This effect dominates the power generation of the foot, which was highest with the intermediate footplate stiffness. Future studies should focus on how tuning footplate stiffness could contribute to optimizing ankle-foot orthosis efficacy in clinical populations.

1. Introduction

In patients with central neurological disorders, lower-limb neuromuscular impairments such as spasticity and (calf) muscle weakness are frequently present. These impairments are often associated with deviations of the gait pattern, e.g. excessive ankle dorsiflexion and knee flexion during stance, excessive plantar flexion and/or reduced ability to push-off (Kempen et al., 2016; Olney, 1996; Ploeger et al., 2017; Rodda et al., 2004). This may contribute to a reduced walking ability in terms of a lower walking speed and/or high energy costs of walking (Brehm et al., 2006; Huang et al., 2015; Kramer et al., 2016; van den Hecke et al., 2007).

Ankle-foot orthoses (AFOs) are commonly prescribed aiming to improve walking ability (CJ and Martina, 2004; Morris et al., 2011). An AFO can improve gait by counteracting excessive muscle activity or compensating a loss of function. AFOs comprising of materials with spring-like properties, e.g. a carbon posterior leaf-spring AFO, are typically prescribed in patients with a reduced ability to push-off during walking. These AFOs can improve the walking ability, by normalizing the ankle and knee joint angles and moments during walking (Bregman et al., 2012; Esposito et al., 2014; Harper et al., 2014; Kerkum et al., 2015a; Kobayashi et al., 2013; Singer et al., 2014; Waterval et al., 2020). Moreover, the spring-like properties of these AFOs allow energy storage in the beginning of the stance phase as a result of ankle dorsal flexion, which is returned during plantar flexion in late stance, thereby taking over or enhancing plantar flexor muscle push off work and enhancing

* Corresponding author at: Agoralaan Gebouw A, 3590 Diepenbeek, Belgium.
E-mail address: yvette.kerkum@uhasselt.be (Y.L. Kerkum).

https://doi.org/10.1016/j.clinbiomech.2021.105422
Received 9 April 2021; Accepted 5 July 2021
Available online 8 July 2021

push-off power (Bregman et al., 2011; Bregman et al., 2012; Kerkum et al., 2015a; Waterval et al., 2020). However, the ankle push-off power generally remains reduced while walking with AFOs relative to normal walking (Bregman et al., 2012; Collins and Kuo, 2010; Esposito et al., 2014; Kerkum et al., 2015a; Kobayashi et al., 2011; Kobayashi et al., 2017a; Kobayashi et al., 2017b).

Several studies in different study populations showed that gait biomechanics and walking ability can be optimized by tuning AFO stiffness around the ankle (Bregman et al., 2012; Collins et al., 2015; Kerkum et al., 2016; Ploeger et al., 2019; Totah et al., 2019; Waterval et al., 2020), e.g. by exchanging posterior leaf springs of different stiffness levels. In addition to the ankle joint, however, the human foot has a significant contribution to push-off power in normal walking (Bruening et al., 2012; Takahashi et al., 2017; Zelik and Honert, 2018). Previous studies indicated deformable behaviour of the foot during stance (Bruening et al., 2012; Leardini et al., 2007), with unique energy and work profiles within the foot structures contributing to both power absorption and generation (Bruening et al., 2012; Kelly et al., 2015; Takahashi et al., 2017; Zelik and Honert, 2018). In addition, the stiffness of the foot segment determines the point of application of the ground reaction force (GRF) during the stance phase of walking, which will affect the mechanical advantage of the actuators around the ankle (Goto and Kumakura, 2013; Landin et al., 2015), and thus the ankle joint moment and power. Yet, it can be argued that the efficacy of the AFO does not only depend on the stiffness of the posterior leaf spring, but also on the properties of the footplate in the AFO. It has already been shown that AFO footplate characteristics can affect lower limb joint angles and moments (Fatone et al., 2009; Kerkum et al., 2015b), yet its effect on push-off power has not been assessed. Although many studies examined the effects of the stiffness properties of the vertical leaf spring of an AFO on ankle push-off power, the potential effects of the stiffness of the footplate on ankle and foot push off power generation are so far largely ignored.

Therefore, the aim of this study was to gain insight in the potential effects of the footplate stiffness of a posterior leaf spring AFO on ankle-foot push-off power. In this study we included healthy participants to explore these mechanical effects in the absence of potentially confounding pathology. It was hypothesized that the AFOs footplate stiffness will affect both the power generated at the ankle joint as well as in the foot segment and consequently total foot-ankle push off power during walking. As such, we would like to demonstrate that the potential benefit of a posterior leaf spring in terms of energy storage and return may be maximized by optimizing footplate stiffness.

2. Methods

2.1. Participants

Twelve healthy participants (7 male, mean (SD) age 24 (Rodda et al., 2004) years; height 175(0) cm; weight 71 (Ploeger et al., 2017) kg) were included in this study. All participants provided written informed consent in accordance with the procedures of the Institutional Review Board of the department of behavioral and movement sciences of VU University (Amsterdam, The Netherlands).

2.2. Materials

The experimental AFO used in this study was a unilateral carbon posterior leaf spring AFO (Ankle7, OttoBock, Duderstadt, Germany), which were aligned in a neutral ankle angle of 0 degrees. To eliminate any interfering effects of the shape of the shoe sole, the AFO was worn in combination with flat flexible sneakers (Fig. 1). The stiffness of the leaf spring was individually selected based on the participant's weight, according to the manufacturer's prescription guidelines. The stiffness of the AFO footplate could be changed by exchanging carbon footplates with different degrees of stiffness, i.e. i) rigid [0.95 Nm·deg.$^{-1}$], ii) stiff (0.45 Nm·deg.$^{-1}$) and iii) flexible (0.04 Nm·deg.$^{-1}$). Footplates extended over the full foot length and were available in different sizes to accommodate to the participant's foot length. The reinforcement was applied uniformly over the whole footplate, where stiffness was changed by using a different amount of carbon layers. Stiffness of the shoe sole [0.02 Nm·deg.$^{-1}$] was found to be negligible. The shoe sole and footplate stiffness were assessed using the Bi-articular Reciprocal Universal Compliance Estimator (BRUCE), which is an instrument designed to define AFO mechanical properties (Bregman et al., 2009).

2.3. Procedure

Participants walked on an instrumented dual belt treadmill with integrated force plate (Sloot et al., 2015) (Ymill, MotekForcelink, Amsterdam, Netherlands) at a fixed speed of 1.25 m·s^{-1}. The first walking trial consisted of a control measurement, i.e. shod walking without the AFO. Thereafter, participants performed three AFO walking conditions, i.e. with the rigid, stiff or flexible footplate, in randomized

Fig. 1. Experimental AFO consisting of a carbon Ankle7 leafspring from which the foot part was shortenend (left panel) and fixed to replaceble footplates with different stiffness levels (middle panel). The leafspring was connected through the back of the shoe to the footplate in a flexible sneaker. The cluster marker on the hindfoot is highlighted (right panel).

order. Each trial started with 2 min of familiarization, followed by 1 min of data recording.

2.4. Measurements

Kinematic data collection was done using a 3D motion capture system (Optotrak, Northern Digital Inc., Waterloo, Canada). Two technical clusters, each consisting of three markers, were rigidly attached to the shoe, at the level of the navicular bone, and shank of the left leg. A pointer was used to indicate the relevant anatomical landmarks on both segments. Anatomical landmarks of the foot that were inside the shoe were pointed on the shoe.

A two-segment model was used, consisting of the shank and hindfoot with articulating ankle joint and a deformable forefoot, i.e. all structures distal to the hindfoot (Bruening et al., 2012; Leardini et al., 2007; Takahashi et al., 2017; Zelik and Honert, 2018). The local reference frame of the shank was defined using the anatomical landmarks of the shank and thigh, i.e. medial and lateral epicondyle of the knee, lateral malleolus and medial malleolus (Kingma et al., 1996). The hindfoot was considered a rigid segment. Its anatomical local reference frame was defined by use of the anatomical landmarks of the calcaneus, medial and lateral malleoli and the point at 50% of the (virtual) line between the anatomical landmarks of the first and fifth distal end of the metatarsal bone during two leg standing pose. Mass and inertial parameters of the structures distal to the hindfoot were neglected. Marker data were tracked at a sample frequency of 100 Hz and synchronized with force plate data.

Ground reaction force data was collected using the integrated force sensors in de separate treadmill belts at a sample frequency 1000 Hz. Spatial calibration of treadmill and motion capture coordinate systems was performed using standard procedures.

2.5. Data processing

Kinematic and force plate data were analyzed using MATLAB version R2015a (The Mathworks, Natick, USA). For each step, segment and joint angles [deg] of the ankle joint and foot segment were determined using Cardan rotation sequences (Kingma et al., 1996). Net joint moments [$\text{Nm}\cdot\text{kg}^{-1}$] around the ankle joint were calculated using inverse dynamics, with respect to the proximal segment's coordinate system. For analysis of potential effects of footplate stiffness of the foot's lever arm during push off, center of pressure (CoP) [m] displacement, defined as the forward displacement of the CoP relative to ankle joint, was calculated.

Anke-foot power [$\text{W}\cdot\text{kg}^{-1}$] calculations were based upon the recommendation of Zelik & Honert (Zelik and Honert, 2018). Following their approach, the mechanical power generated by the different structures of the ankle and foot complex was subdivided into two components; the ankle joint complex power (P_{AJC}) and distal hindfoot power (P_{DHF}) (Zelik and Honert, 2018). P_{AJC} describes the interaction between the shank and the hindfoot and provides an estimate of the contribution of the muscles crossing the ankle joint and the posterior leaf spring which ends at the posterior side of the calcaneus in the back of the shoe. P_{DHF} describes the power due to 6 degrees of freedom motion of the defined hindfoot segment relative to the ground, as such reflecting the combined power from all structures distal to this segment. This approach has been shown to be more robust to the deformation occurring in the foot than the conventional modelling of the foot with a rigid toe segment and hinge joint (Zelik and Honert, 2018).

P_{AJC} was calculated as:

$$P_{AJC} = \vec{F}ank\bullet(\vec{v}\text{ank, shank} - \vec{v}\text{ank,hf}) + \vec{M}\text{ank}\bullet(\vec{\omega}\text{shank} - \vec{\omega}\text{hf}) \tag{1}$$

in which, $\vec{F}ank$ is the net ankle force on the shank segment. $\vec{v}ank, shank$ and $\vec{v}ank, hf$ respectively the velocity of the ankle joint center based on rigid body motion of the shank and hindfoot. $\vec{M}ank$ is the ankle joint moment and $\vec{\omega}shank$ and $\vec{\omega}hf$ respectively the angular velocity of the shank and the hindfoot, indicated as the relative angular velocity of the shank with respect to the hindfoot.

P_{DHF} was calculated as:

$$P_{DHF} = \vec{F}grf\bullet\left(\vec{v}\text{hf} + \vec{\omega}\text{hf} \times \vec{r}\text{cop}/_{\text{hf}}\right) + \vec{M}\text{free}\bullet\vec{\omega}\text{hf} \tag{2}$$

in which, $\vec{F}grf$ is the ground reaction force, $\vec{v}hf$ is the velocity of the hindfoot Center of Mass (CoM) and $\vec{\omega}hf$ is the rotation velocity of the hindfoot segment. $\vec{r}cop/hf$ is the position of the CoP relative to the hindfoot CoM and $\vec{M}free$ is the free moment exerted on the force plate (Zelik et al., 2015).

P_{AJC} and P_{DHF} were added up into total ankle-foot power (P_{TAF}), i.e. the power generation of the combined ankle-foot.

$$P_{TAF} = P_{AJC} + P_{DHF} \tag{3}$$

From the power profiles during the stance phase, positive and negative mechanical work [$\text{J}\cdot\text{kg}^{-1}$] of the ankle joint complex (W_{AJC}), hindfoot (W_{DHF}) were calculated by taking the integral over the positive and negative power interval during stance phase, and added up into positive and negative total ankle-foot mechanical work (W_{TAF}).

Peak power and work were calculated for all stance phases of the leg wearing the AFO during the final minute of each trial. Stance phase was defined from heel strike to toe off (GRF > 25 N). All outcome variables were averaged over all correctly recorded strides during the 1-min data acquisition. For graphical representation, power profiles were time normalized to 100% stance phase before averaging.

2.6. Statistics

Statistical analyses were done with SPSS version 20 (SPSS Inc., Chicago, USA), using an alpha level of 0.05 for all tests of significance. Descriptive statistics (mean and standard error (SE)) were used to summarize all outcomes parameters. Differences in outcome parameters between conditions were analyzed using a repeated measures ANOVA, with conditions (i.e. shod walking, and rigid, stiff and flexible footplate stiffness) as within-subject factor. Differences between individual conditions were determined post-hoc using a Bonferroni correction. The non-parametric Friedman's test was used for data which were not normally distributed. In that case, differences between individual conditions were determined post-hoc using Wilcoxon signed- rank test with Bonferroni adjustments (0.05/n-analysis).

3. Results

3.1. Power and mechanical work

Significant main effects were found for all joint power components. The peak P_{AJC} was highest in shod condition and in the AFO condition with rigid footplate, and significantly lower while walking with the flexible and stiff footplate. Peak P_{DHF} was highest while walking with the stiff footplate, and differed significantly from shod walking and walking with the flexible footplate. Peak total ankle and foot power (P_{TAF}) increased with increasing footplate stiffness. Peak P_{TAF} was significantly different between successive footplate stiffness conditions and significantly lower while walking with the flexible footplate compared to shod walking (Table 1; Fig. 2).

Changes in power profiles as a result of foot plate stiffness were also reflected in positive and negative mechanical work during the stance phase. Positive W_{AJC} was significantly higher during shod walking and while walking with the rigid footplate compared to both walking with the flexible and stiff footplate. Positive W_{DHF} was significantly higher with the stiff footplate compared to all other walking conditions.

Table 1
Effects of different walking conditions on mean (SD) peak ankle-foot power and mechanical work during stance (n = 12).

		Condition				Statistics		
		Shod	Flexible	Stiff	Rigid	F	*p*	Post-hoc
P_{AJC}	*[W·kg^{-1}]*	2.57 (0.654)	1.41 (0.358)	1.38 (0.312)	2.24 (0.382)	26.9	<0.001	sh-f; sh-s; f-r; s-r;
P_{DHF}	*[W·kg^{-1}]*	0.63 (0.184)	0.62 (0.192)	0.87 (0.134)	0.74 (0.233)	9.04	<0.001	sh-s; f-s
P_{TAF}	*[W·kg^{-1}]*	2.41 (0.665)	1.48 (0.210)	1.96 (0.231)	2.69 (0.406)	22.5	<0.001	sh-f; f-s; f-r; s-r;
positive W_{AJC}	*[J·kg^{-1}]*	25.2 (7.65)	15.6 (4.00)	17.4 (4.03)	25.3 (5.07)	13.6	0.001	sh-f; sh-s; f-r; s-r
negative W_{AJC}	*[J·kg^{-1}]*	−29.2 (10.60)	−28.2 (5.67)	−30.6 (7.71)	−33.2 (4.55)	1.94	0.142	
positive W_{DHF}	*[J·kg^{-1}]*	7.7 (2.94)	8.9 (1.74)	10.9 (1.68)	7.7 (1.93)	9.60	<0.001	sh-s; f-s; s-r
negative W_{DHF}	*[J·kg^{-1}]*	−9.1 (4.03)	−13.3 (4.50)	−13.5 (5.47)	−12.4 (2.45)	3.08	0.041	
positive W_{TAF}	*[J·kg^{-1}]*	27.3 (6.81)	17.0 (3.05)	21.3 (3.52)	28.7 (4.43)	16.6	<0.001	sh-f; f-s; f-r; s-r
negative W_{TAF}	*[J·kg^{-1}]*	−32.5 (10.20)	−34.1 (6.34)	−37.8 (5.62)	−41.1 (5.69)	6.55	0.001	sh-r; f-r;

Abbreviations: f, flexible footplate; P_{AJC}, ankle joint center power; P_{DHF}, distal hindfoot power; P_{TAF}, total ankle-foot power; r, rigid footplate; s, stiff footplate; sh, shod walking; W_{AJC}, ankle joint center work; W_{DHF}, distal hindfoot work; W_{TAF}, total ankle-foot work.

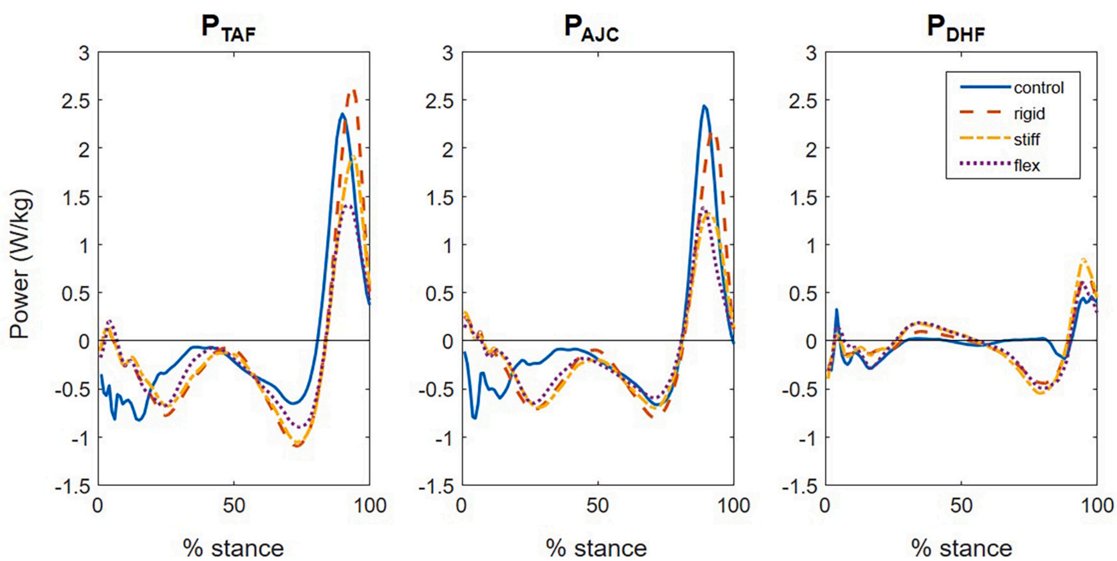

Fig. 2. Mean ($n = 12$) power of different structures of the ankle and foot during walking, normalized to 100% stance phase, for different walking conditions. Panels represent total ankle-foot power (P_{TAF}), ankle joint complex power (P_{AJC}) and distal hind foot power (P_{DHF}). Control (blue) represents shod walking, rigid (red), stiff (yellow), and flex (purple) represent walking with a rigid, stiff and flexible AFO footplate stiffness, respectively. (For interpretation of the references to colour in this figure legend, the reader is referred to the web version of this article.)

Positive W_{TAF} again increased with footplate stiffness. It was significantly higher in all condition compared to walking with flexible footplate, and significantly higher with the rigid footplate compared to the stiff footplate condition. No significant effects in negative mechanical work were found for AJC and DHF, but negative W_{TAF} was significantly higher in the rigid footplate condition compared to all other walking conditions (Table 1).

3.2. Secondary parameters

The ankle joint peak plantar flexion angle and ankle RoM were significantly larger for shod walking compared to all footplate stiffness conditions, but showed no significant difference between footplate stiffness. Peak ankle dorsal flexion was largest while walking with the rigid footplate but only differed significantly from shod walking. Net ankle internal plantarflexion moment increased with foot plate stiffness and was significantly different between successive footplate stiffness conditions. Net ankle plantarflexion moment was also significantly

Table 2
Effects of different walking conditions on mean (SD) peak ankle joint kinematics and kinetics during stance (n = 12).

		Condition				Statistics		
		Shod	Flexible	Stiff	Rigid	F	*p*	Post-hoc
Dorsal flexion angle	*[deg]*	−3.0 (5.06)	−4.8 (3.78)	−4.5 (3.44)	−6.0 (4.35)	3.65	<0.022	sh-r;
Plantar flexion angle	*[deg]*	19.0 (4.50)	5.4 (3.30)	5.4 (2.69)	4.6 (3.28)	117	<0.001	sh-f; sh-s; sh-r;
RoM *	*[deg]*	21.9 (2.51)	9.4 (2.09)	9.9 (1.91)	10.3 (1.71)	181	<0.001	sh-f; sh-s; sh-r;
ω ankle	*[deg·s^{-1}]*	213.6 (66.9)	68.5 (20.95)	75.5 (22.18)	73.0 (23.26)	44	<0.001	sh-f; sh-s; sh-r
net ankle moment [a]	*[Nm·kg^{-1}]*	1.43 (0.149)	1.39 (0.104)	1.49 (0.122)	1.64 (0.106)	19	<0.001	sh-r; f-s; f-r; s-r
CoP displacement	*[m]*	0.13 (0.013)	0.13 (0.011)	0.13 (0.012)	0.14 (0.007)	9.7	<0.002	sh-r; f-r; s-r

* non- parametric, F = χ^2.
[a] *internal plantarflexion moment.*
Abbreviations: CoP, center of pressure; f, flexible footplate; r, rigid footplate; RoM, range of motion; s, stiff footplate; sh, shod walking; ω ankle, ankle angular velocity.

higher in the rigid footplate condition compared to shod walking (Table 2; Fig. 3).

Compared to shod walking, ankle angular velocity was significantly decreased while walking with AFOs, showing no effects of footplate stiffness (Table 2). A significant main effect was found for CoP displacement. Post-hoc analyses revealed that CoP displacement was larger while walking with the rigid footplate compared all other walking conditions (Table 2; Fig. 3).

4. Discussion

The aim of this study was to gain insight into the effects of footplate stiffness on ankle-foot push-off power in able-bodied persons while walking with a posterior leaf spring AFO. Our results showed that footplate stiffness significantly affects ankle-foot power generation. Furthermore, power generated by the ankle joint complex (P_{AJC}) and the hindfoot (P_{DHF}) were affected by the footplate stiffness in distinctly different ways.

Our analyses allowed evaluation of the power contributions from structures around the ankle joint, i.e. plantarflexor muscle-tendon and AFO leaf spring, as well as structures around the foot, including the AFO's footplate (Zelik and Honert, 2018). Separate contributions of the ankle joint complex and distal hindfoot to total ankle-foot power were comparable to studies on barefoot walking in healthy people (Bruening et al., 2012; Takahashi et al., 2017; Zelik and Honert, 2018), showing that P_{AJC} is the most important contributor to mechanical power generation during push-off (Table 1; Fig. 2). P_{AJC} was higher while walking with rigid footplate, compared the flexible and stiff footplate (Table 1; Fig. 2). The significant increase of the forward CoP displacement with increasing footplate stiffness (Table 2; Fig. 3) indicates that the rigid footplate introduced a larger lever arm of the GRF to the ankle joint rotation center compared to the other footplates. This coincided with an increased plantarflexion moment while walking with the rigid footplate compared to all other walking conditions (Table 2; Fig. 3). Although we cannot differentiate between contribution of the calf muscles and the posterior leaf spring in our analysis, it can be argued that this increased plantar flexor moment will put more load on the posterior leaf spring exploiting its energy storing capacity to a larger extent. Yet, our results confirm that altering footplate stiffness changes the point of application of the GRF relative to the ankle joint (Eddison and Chockalingam, 2013; Kerkum et al., 2015b), therewith affecting the mechanical advantage of the actuators around the ankle (Goto and Kumakura, 2013; Landin et al., 2015), including the AFO's posterior leaf spring.

Next to the P_{AJC}, the power generated in the foot (P_{DHF}) has a meaningful contribution to total ankle-foot push-off power (Table 1; Fig. 2). Stiffness of the AFO footplate affects the amount of work absorbed and subsequently generated in the foot segment. P_{DHF} was found to be highest when walking with the stiff footplate compared to all other walking conditions, although not significantly different compared to the rigid footplate (Table 1; Fig. 2). Previous research found that the energy-storing capacity of carbon AFO parts is stiffness dependent, being optimal for medium stiffness degrees (Bregman et al., 2011). Accordingly, the mechanical properties of the stiff footplate seem to enhance energy storage and return as reflected in highest P_{DHF} and W_{DHF}. Notably, although the amount of energy that can be returned by the footplate is low compared to the capacity of the AFO's leaf spring, the difference in total ankle-foot power between walking with the stiff and flexible footplate seems to originate mainly from power contribution of the foot.

Compared to shod walking, total ankle-foot push-off power was significantly reduced while walking with an AFO using a flexible and stiff footplate (Table 1; Fig. 2). This reduction of ankle push-off power was a consequence of a reduced ankle RoM and angular velocity induced by the AFO, and is in accordance to previous findings (Bregman et al., 2012; Esposito et al., 2014; Kerkum et al., 2015a; Kobayashi et al., 2017a). Previous studies suggested and showed that this limiting effect of AFOs on ankle range of motion and hence push-off power and ankle work can be minimized by optimizing the AFO stiffness around the ankle joint (Bregman et al., 2012; Kerkum et al., 2015a; Ploeger et al., 2019; Waterval et al., 2020). However, these studies did not consider footplate stiffness in their study design. Our results indicate that footplate stiffness is an important parameter to tune when optimizing AFO properties. With the rigid footplate we could enhance ankle and foot push off power to the level of shod walking while using a fixed posterior leaf spring stiffness in our able-bodied participants. Therefore, future studies should focus on optimizing the combined effects of the AFO's ankle and footplate stiffness, therewith further maximizing treatment efficacy.

This study is subject to some limitations. In this study, the marker cluster at the hindfoot was attached to the shoe. Due to possible movement of the foot and AFO in the shoe during push-off, an underestimation in hindfoot motion may have occurred, resulting in deviations in power attributed to AJC or DHF. Nevertheless, total ankle-foot power would not be affected. This was checked by calculating distal shank power (Zelik and Honert, 2018), which provided similar

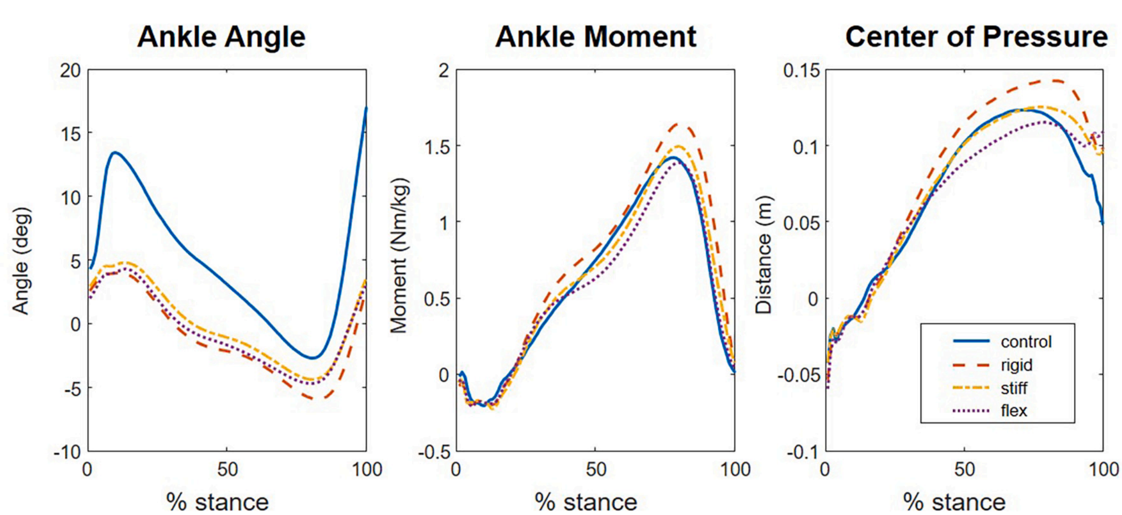

Fig. 3. Mean (n = 12) sagittal ankle angle, internal ankle flexion-extension moment, and center of pressure displacement for different walking conditions, normalized to 100% stance phase. Control (blue) represents shod walking, rigid (red), stiff (yellow), and flex (purple) represent walking with a rigid, stiff and flexible AFO footplate stiffness, respectively. Positive values on the y-axis of ankle angle and ankle moment represent plantar flexion. (For interpretation of the references to colour in this figure legend, the reader is referred to the web version of this article.)

results to P_{TAF}. We only manipulated AFO stiffness in this study, while other properties are also relevant for AFO treatment efficacy, e.g. alignment of the shank in the AFO-footwear combination. We used a neutral (zero degree) alignment of the AFO-footwear combination throughout our experiments. Studies have shown that individualized tuning of the alignment of the AFO-footwear combination, i.e. a shank-to-vertical angle of 8–12 degrees, is a prerequisite for optimal AFO efficacy (20, 34, 35). We did not tune this parameter in our population but assume effect to be randomly distributed over conditions between participants. Furthermore, we only evaluated effects of footplate stiffness on ankle and foot parameters, while changes in footplate stiffness and concomitant shifts in COP displacement can also affect alignment of the GRF relative to the knee joint (Fatone et al., 2009; Kerkum et al., 2015b). Most importantly, our study was conducted in able-bodied persons to observe the biomechanical effects of footplate stiffness in the absence of movement pathology. While these biomechanical effects will also apply to patient populations, their specific pathology might mediate to an overall effect. As our results cannot be generalized to patients with movement pathologies, future research should focus on clinical target populations and include the effects of changing AFO footplate stiffness on both foot, ankle and the knee joint.

5. Conclusions

In conclusion, the push off power during walking with a posterior leaf spring AFO is dependent on footplate stiffness. Stiffness of the footplate affects the lever arm of the GRF, thereby increasing the ankle joint moment and power generation. This can result in higher storage and release of mechanical power in the posterior leaf spring and as such enhance efficacy of the AFO. In addition, AFO footplate stiffness affects the amount of energy stored and released in the foot segment, although this effect is smaller compared to the effect at the level of the ankle. We propose that tuning of footplate stiffness should be considered in concert with tuning of the posterior leaf spring stiffness when optimizing AFO treatment in clinical practice. Future studies should address this issue in different patient populations.

Declaration of competing interest

The authors declare the following financial interests/personal relationships which may be considered as potential competing interests: Yvette Kerkum was employed by OIM Orthopedie by the time this study was performed. Neither OIM Orthopedie, nor Yvette Kerkum have (financial) benefits related to this project. There are no other conflicts of interest associated with this study.

Acknowledgements

The authors would like to thank OIM Orthopedie (Assen, The Netherlands) for providing the leaf springs and manufacturing the AFOs with different footplates.

References

Bregman, D.J., Rozumalski, A., Koops, D., de Groot, V., Schwartz, M., Harlaar, J., 2009. A new method for evaluating ankle foot orthosis characteristics: BRUCE. Gait Posture 30 (2), 144–149.
Bregman, D.J., van der Krogt, M.M., de Groot, V., Harlaar, J., Wisse, M., Collins, S.H., 2011. The effect of ankle foot orthosis stiffness on the energy cost of walking: a simulation study. Clin. Biomech. 26 (9), 955–961.
Bregman, D.J., Harlaar, J., Meskers, C.G., de Groot, V., 2012. Spring-like ankle foot orthoses reduce the energy cost of walking by taking over ankle work. Gait Posture 35 (1), 148–153.
Brehm, M.A., Nollet, F., Harlaar, J., 2006. Energy demands of walking in persons with postpoliomyelitis syndrome: relationship with muscle strength and reproducibility. Arch. Phys. Med. Rehabil. 87 (1), 136–140.
Bruening, D.A., Cooney, K.M., Buczek, F.L., 2012. Analysis of a kinetic multi-segment foot model part II: kinetics and clinical implications. Gait Posture 35 (4), 535–540.
Report of a consensus conference on the orthotic management of stroke patients. In: CJ, Condie E., Martina, J. (Eds.), 2004. International Society for Prosthetics and Orthotics. Copenhagen.
Collins, S.H., Kuo, A.D., 2010. Recycling energy to restore impaired ankle function during human walking. PLoS One 5 (2), e9307.
Collins, S.H., Wiggin, M.B., Sawicki, G.S., 2015. Reducing the energy cost of human walking using an unpowered exoskeleton. Nature. 522 (7555), 212–215.
Eddison, N., Chockalingam, N., 2013. The effect of tuning ankle foot orthoses-footwear combination on the gait parameters of children with cerebral palsy. Prosthetics Orthot. Int. 37 (2), 95–107.
Esposito, E.R., Blanck, R.V., Harper, N.G., Hsu, J.R., Wilken, J.M., 2014. How does ankle-foot orthosis stiffness affect gait in patients with lower limb salvage? Clin. Orthop. Relat. Res. 472 (10), 3026–2036.
Fatone, S., Gard, S.A., Malas, B.S., 2009. Effect of ankle-foot orthosis alignment and foot-plate length on the gait of adults with poststroke hemiplegia. Arch. Phys. Med. Rehabil. 90 (5), 810–818.
Goto, R., Kumakura, H., 2013. The estimated mechanical advantage of the prosimian ankle joint musculature, and implications for locomotor adaptation. J. Anat. 222 (5), 538–546.
Harper, N.G., Esposito, E.R., Wilken, J.M., Neptune, R.R., 2014. The influence of ankle-foot orthosis stiffness on walking performance in individuals with lower-limb impairments. Clin. Biomech. 29 (8), 877–884.
Huang, T.W., Shorter, K.A., Adamczyk, P.G., Kuo, A.D., 2015. Mechanical and energetic consequences of reduced ankle plantar-flexion in human walking. J. Exp. Biol. 218 (Pt 22), 3541–3550.
Kelly, L.A., Lichtwark, G., Cresswell, A.G., 2015. Active regulation of longitudinal arch compression and recoil during walking and running. J. R. Soc. Interface 12 (102), 20141076.
Kempen, J.C., Doorenbosch, C.A., Knol, D.L., de Groot, V., Beckerman, H., 2016. Newly identified gait patterns in patients with multiple sclerosis may be related to push-off quality. Phys. Ther. 96 (11), 1744–1752.
Kerkum, Y.L., Buizer, A.I., van den Noort, J.C., Becher, J.G., Harlaar, J., Brehm, M.A., 2015a. The effects of varying ankle foot orthosis stiffness on gait in children with spastic cerebral palsy who walk with excessive knee flexion. PLoS One 10 (11), e0142878.
Kerkum, Y.L., Houdijk, H., Brehm, M.A., Buizer, A.I., Kessels, M.L., Sterk, A., et al., 2015b. The shank-to-vertical-angle as a parameter to evaluate tuning of ankle-foot orthoses. Gait Posture 42 (3), 269–274.
Kerkum, Y.L., Harlaar, J., Buizer, A.I., van den Noort, J.C., Becher, J.G., Brehm, M.A., 2016. An individual approach for optimizing ankle-foot orthoses to improve mobility in children with spastic cerebral palsy walking with excessive knee flexion. Gait Posture 46, 104–111.
Kingma, I., de Looze, M.P., Toussaint, H.M., Klijnsma, H.G., Bruijnen, T.B.M., 1996. Validation of a full body 3-D dynamic linked segment model. Hum. Mov. Sci. 15 (6), 833–860.
Kobayashi, T., Leung, A.K., Akazawa, Y., Hutchins, S.W., 2011. Design of a stiffness-adjustable ankle-foot orthosis and its effect on ankle joint kinematics in patients with stroke. Gait Posture 33 (4), 721–723.
Kobayashi, T., Leung, A.K., Akazawa, Y., Hutchins, S.W., 2013. The effect of varying the plantarflexion resistance of an ankle-foot orthosis on knee joint kinematics in patients with stroke. Gait Posture 37 (3), 457–459.
Kobayashi, T., Orendurff, M.S., Hunt, G., Lincoln, L.S., Gao, F., LeCursi, N., et al., 2017a. An articulated ankle-foot orthosis with adjustable plantarflexion resistance, dorsiflexion resistance and alignment: a pilot study on mechanical properties and effects on stroke hemiparetic gait. Med. Eng. Phys. 44, 94–101.
Kobayashi, T., Orendurff, M.S., Singer, M.L., Gao, F., Foreman, K.B., 2017b. Contribution of ankle-foot orthosis moment in regulating ankle and knee motions during gait in individuals post-stroke. Clin. Biomech. 45, 9–13.
Kramer, S., Johnson, L., Bernhardt, J., Cumming, T., 2016. Energy expenditure and cost During walking after stroke: a systematic review. Arch. Phys. Med. Rehabil. 97 (4), 619–632 e1.
Landin, D., Thompson, M., Reid, M., 2015. Knee and ankle joint angles influence the plantarflexion torque of the gastrocnemius. J. Clin. Med. Res. 7 (8), 602–606.
Leardini, A., Benedetti, M.G., Berti, L., Bettinelli, D., Nativo, R., Giannini, S., 2007. Rear-foot, mid-foot and fore-foot motion during the stance phase of gait. Gait Posture 25 (3), 453–462.
Morris, C., Bowers, R., Ross, K., Stevens, P., Phillips, D., 2011. Orthotic management of cerebral palsy: recommendations from a consensus conference. NeuroRehabilitation 28 (1), 37–46.
Olney, S.J., 1996. Hemiparetic gait following stroke. Part I: characteristics. Gait Posture 4, 136–148.
Ploeger, H.E., Bus, S.A., Nollet, F., Brehm, M.A., 2017. Gait patterns in association with underlying impairments in polio survivors with calf muscle weakness. Gait Posture 58, 146–153.
Ploeger, H.E., Waterval, N.F.J., Nollet, F., Bus, S.A., Brehm, M.A., 2019. Stiffness modification of two ankle-foot orthosis types to optimize gait in individuals with non-spastic calf muscle weakness - a proof-of-concept study. J. Foot Ankle Res. 12, 41.
Rodda, J.M., Graham, H.K., Carson, L., Galea, M.P., Wolfe, R., 2004. Sagittal gait patterns in spastic diplegia. J. Bone Joint Surg. (Br.) 86 (2), 251–258.
Singer, M.L., Kobayashi, T., Lincoln, L.S., Orendurff, M.S., Foreman, K.B., 2014. The effect of ankle-foot orthosis plantarflexion stiffness on ankle and knee joint kinematics and kinetics during first and second rockers of gait in individuals with stroke. Clin. Biomech. 29 (9), 1077–1080.
Sloot, L.H., Houdijk, H., Harlaar, J., 2015. A comprehensive protocol to test instrumented treadmills. Med. Eng. Phys. 37 (6), 610–616.

Takahashi, K.Z., Worster, K., Bruening, D.A., 2017. Energy neutral: the human foot and ankle subsections combine to produce near zero net mechanical work during walking. Sci. Rep. 7 (1), 15404.

Totah, D., Menon, M., Jones-Hershinow, C., Barton, K., Gates, D.H., 2019. The impact of ankle-foot orthosis stiffness on gait: a systematic literature review. Gait Posture 69, 101–111.

van den Hecke, A., Malghem, C., Renders, A., Detrembleur, C., Palumbo, S., Lejeune, T. M., 2007. Mechanical work, energetic cost, and gait efficiency in children with cerebral palsy. J. Pediatr. Orthop. 27 (6), 643–647.

Waterval, N.F.J., Brehm, M.A., Altmann, V.C., Koopman, F.S., Den Boer, J.J., Harlaar, J., et al., 2020. Stiffness-optimized ankle-foot orthoses improve walking energy cost compared to conventional orthoses in neuromuscular disorders: a prospective uncontrolled intervention study. IEEE Trans. Neur. Syst. Rehab. Eng. 28 (10), 2296–2304.

Zelik, K.E., Honert, E.C., 2018. Ankle and foot power in gait analysis: implications for science, technology and clinical assessment. J. Biomech. 75, 1–12.

Zelik, K.E., Takahashi, K.Z., Sawicki, G.S., 2015. Six degree-of-freedom analysis of hip, knee, ankle and foot provides updated understanding of biomechanical work during human walking. J. Exp. Biol. 218 (Pt 6), 876–886.